PROCEEDINGS OF SCIENCE

# Excitation Functions of (p,n) Reactions on $^{115, 116, 120}$Sn

**Ye. Skakun***
*National Science Center „Kharkiv Institute of Physics and Technology“*
*Academicheskaja str., 1, 61108 Kharkiv, Ukraine*
*E-mail:* skakun@kipt.kharkov.ua

**T. Rauscher**
*Departement für Physik und Astronomie, Universität Basel*
*Klingelbergstr, 82, CH-4056 Basel, Switzerland*
*E-mail:* Thomas.Rauscher@unibas.ch

Using the activation technique (p,n)-reaction cross sections of the tin isotopes with *A*=115, 116 and 120, the first of which is a *p*-process isotope, have been measured in the proton energy range between 4.5 and 9.0 MeV, corresponding to stellar temperatures $T_9 > 3$. Thin self-supporting foils of enriched tin isotopes were irradiated at the Kharkiv linear accelerator with proton beam intensities of (100…150) nA. The induced activities were measured with a calibrated Ge(Li)-detector. The cross sections for the production of isomeric states in $^{116}$Sb ($J_m=8^-$, $J_g=3^+$) and $^{120}$Sb ($J_m=8^-$, $J_g=1^+$) were determined separately. The total cross sections of the $^{120}$Sn(p,n)$^{120}$Sb reaction are compared with the results of other authors obtained with the neutron counting technique in this incident proton energy range. The cross sections, astrophysical S-factors, and reaction rates derived from the experiment are compared with Hauser-Feshbach statistical theory predictions. In general, good agreement is found.

*International Symposium on Nuclear Astrophysics – Nuclei in the Cosmos – IX*
*CERN, Geneva, Switzerland*
*25-30 June, 2006*

* Speaker

 

PoS(NIC-IX)204

## 1. Introduction

The majority of the natural isotopes of intermediate and heavy elements were synthesized in stars via slow (*s*) and rapid (*r*) processes of neutron capture and following $\beta^-$-decays [1]. Proton and $\alpha$-particle induced reactions occur in hydrostatic stellar burning but are more relevant for lighter elements due to the Coulomb barrier hampering charged particle reactions with heavier targets. However, the inverse process to capture—photodisintegration—can release charged particles in hot stellar environments and thus produce proton-rich isotopes. Thus, stellar nucleosynthesis creates elements from decays of radioactive nuclei from both the left and right side of the valley of stability. For example, there are 32 stable isotopes in the mass number region $74 \leq A \leq 196$ shielded from the direction of neutron rich radioactive nuclei which can be solely synthesized in the so-called *p*-process. At typical temperatures of $(2\text{-}3)\times 10^9$ Kelvin (K), a complicated sequence of $\gamma$-dissociation processes as well as p- and $\alpha$-particle induced reactions below the Coulomb barrier contribute to the nucleosynthetic yields, producing neutron deficient nuclei.

There are several compilations of both experimental [cf. 2, 3] and theoretical [4] nuclear reaction cross sections needed for astrophysical simulations, covering the temperature range up to $T=10^{10}$ K, corresponding to proton bombarding energies of about 8 MeV in the tin region. The scarcity of available experimental data and the necessity to know reaction cross sections of a multitude of radioactive nuclei at low energies, which cannot be measured at laboratory conditions, underline the significance of theoretical calculations. The statistical model of Hauser-Feshbach (H-F) is usually used for this aim. There are computer codes [5,6,7] implementing H-F theory which are especially tailored for the calculation of astrophysical cross sections and reaction rates.

New experimental nuclear reaction cross sections are required for data compilations used in the simulation of nucleosynthesis scenarios and to help the further development of theories and model parameterizations. Even though reactions induced by the charged particles released in the *p*-process photodisintegration may only be important in a short freeze-out phase, they can be used as an independent test of the applied cross section predictions. Moreover, information can also be obtained about the reverse reaction by applying detailed balance. Using the activation technique, we have earlier [8] carried out measurements of the excitation functions of the reactions $^{115}Sn(p,n)^{115}Sb$ (Q=-3.81 MeV), $^{116}Sn(p,n)^{116m,g}Sb$ ($Q_g$=-5.49 MeV) and $^{120}Sn(p,n)^{120m,g}Sb$ ($Q_g$=-3.46 MeV) in the incident proton energy region (4.5 - 9.0) MeV, revised the data anew (see next part) and compared them with the results obtained by means of the computer code NON-SMOKER [6] of H-F statistical theory. Among the targets investigated, $^{115}Sn$ is a *p*-process isotope. The Gamow window for the proton reactions on tin isotopes is (3.7±1.2) MeV at the stellar temperature of $3.3\times10^9$ K. Thus, the energy range of our measurements corresponds to slightly higher temperature values due to the negative Q-values of these reactions. For the reaction $^{120}Sn(p,n)^{120}Sb$ known literature data of other authors at the lower bombarding energies are included in the analysis. The astrophysical S-factors and rates were deduced from the total ($\sigma=\sigma_m+\sigma_g$) cross section values of the reactions investigated to test the applicability of the statistical model.

TABLE 1. Enrichment of tin target material (in percent)

| **Mass** | 112 | 114 | 115 | 116 | 117 | 118 | 119 | 120 | 122 | 124 |
|---|---|---|---|---|---|---|---|---|---|---|
| 115 | 0,1 | 1,46 | **51,2** | 24,36 | 5,37 | 7,36 | 1.94 | 6,68 | 0,74 | 0,79 |
| 116 | 0,1 | | 0,2 | **92,8** | 3,7 | 2,5 | 0,2 | 0,6 | 0,1 | |
| 120 | 0,05 | | | | 0,4 | 0,6 | 2,5 | **96,5** | 0,1 | |

## 2. Experiment

To measure the cross sections of the (p,n)-reactions studied here, the targets were irradiated with the beam of the proton linear accelerator of the Kharkiv Institute of Physics and Technology. The self-supporting metallic foils of (3-6) mg $cm^{-2}$ thickness and 22 mm diameter made from enriched tin isotopes (supplied by the State Fund of Stable Isotopes, Russia) by the electrolytic deposition technique [9] were employed in the experiment. Enrichment and major contaminants of the targets are listed in Table 1. The targets were mounted at the bottom of a Faraday cup with secondary electron suppression. The proton energy was decreased with pure aluminum foils-absorbers and, within small limits, also by the method of energy variation of linear accelerator beams developed at NSC KIPT [10]. Thinner target foils were irradiated at the lower incident proton energies to supply smaller energy losses. The energy losses in the Al-absorbers and studied tin targets were determined by a code calculating the energy degradation using the range-energy relation [11]. The total uncertainty in each proton energy determined as a root-mean-square value of the individual uncertainties of the initial proton energy (up to 100 keV) and of degradation in the foils did not exceed 130 keV. The beam current was measured with the charge integrator and typically amounted to 100-150 nA. The length of irradiation depended on the half-life of the residual nucleus studied and was chosen to be equal to about $3T_{1/2}$. The foils were irradiated one by one in the majority of cases since the residual nuclei have half-lives comparable to the irradiation and measurement time. Additional measurements were made for the production cross sections of the long-lived $^{120m}Sb$ isomer, using a stack of foils sandwiched between thin Al absorbers and irradiating them with the maximum energy proton beam. The irradiation time for this case was lengthened to 8 hours. The beam current incident upon the Faraday cup was recorded in small time intervals in order to be able to account for beam fluctuations in the later off-line activity measurements and the cross section determination.

The activity of each irradiated target was measured with a Ge(Li) detector located at a low background counting area far from the accelerator. The targets were placed at a distance assuring a low dead time (<4%). The absolute efficiency of the detector was measured with standard $^{22}Na$, $^{57}Co$, $^{60}Co$, $^{65}Zn$, $^{88}Y$, $^{113}Sn$, $^{137}Cs$, $^{139}Ce$, $^{241}Am$ sources in the same geometry as used for the measurements. The half-lives, energies and branching ratios of the strongest γ-transitions following the β-decay of the produced Sb isotopes are listed in Table 2 [12].

Experimental cross sections of the reactions studied were derived using the activation equation, taking into account the decay of activity during irradiation, cooling and measurement time. The measurement time was usually chosen to be equal to the irradiation time. The typical total root-mean-squared uncertainty of each experimental cross section resulting from all individual errors (the surface density of target nuclei, incident proton beam current, detector efficiency, counting statistics and decay data) was in the range (7-13)%, except at the lowest energy point for the reaction $^{116}$Sn(p,n)$^{116}$Sb for which it exceeded 30%. The estimates made by means of some known experimental values of (p,γ)-reaction cross sections on tin isotopes [13, 14] and theoretical calculations show negligible contribution to activities from radiative capture on the contaminants of our enriched targets.

The review of current radioactive nuclei decay data bases (ENSDF, NUDAT, TOI [12] ) shows the good agreement with the Brown and Firestone [15] compilation used in [8], except for the $^{120g}$Sb nuclei, the yield of which gives the main contribution in the total cross section of the $^{120}$Sn(p,n)$^{120}$Sb-reaction. Adoption of a new branching ratio for the 1171 keV γ-transition (the last line of Table 2) gives the cross section values 11.8(2.1), 34.9(4.1), 66.0(7.7), 118(14), 164(18), 212(33), 263(30), 354(39), and 375(42) millibarns at the incident proton energies 5.0, 5.5, 6.0, 6.5, 7.0, 7.5, 8.0, 8.5, and 9.0 MeV, respectively, for the reaction $^{120}$Sn(p,n)$^{120g}$Sb which we used in the present analysis.

TABLE 2. Spectroscopic data of residual antimony nuclei used in the data analysis

| **Isotope** | **Half-life** | **$E_\gamma$, keV** | **$I_\gamma(\Delta I_\gamma)$ , %** |
|---|---|---|---|
| $^{115}$Sb | 32.1 min | 497 | 97.9(0.4) |
| $^{116m}$Sb | 60.3 min | 543 | 48.1(4.1) |
| | | 972 | 74.2(4.1) |
| | | 1072 | 25.5(4.2) |
| | | 1293 | 100(4.1) |
| $^{116g}$Sb | 15.8 min | 932 | 24.9(1.9) |
| | | 1293 | 84.8(6.3) |
| $^{120m}$Sb | 5.76 d | 197 | 87.0(1.1) |
| | | 1023 | 99.4(0.3) |
| | | 1171 | 100 |
| $^{120g}$Sb | 15.89 min | 1171 | 1.69(0.09) |

## 3. Results and Discussion

The results of our investigations are presented in Figure 1. In the left column the excitation functions of the reactions $^{115}$Sn(p,n)$^{115}$Sb, $^{116}$Sn(p,n)$^{116m+g}$Sb and $^{120}$Sn(p,n)$^{120m+g}$Sb are shown. The sums of the production cross sections of isomer and ground state are plotted for the last two reactions. The experimental values of the cross sections (in millibarns) are given by the points with errors, while the theoretical ones calculated with the NON-SMOKER code [6] are depicted by curves. On the whole, good agreement of the predictions with our experimental cross section values is observed. The data of other authors found in literature are included in plot *c* for the $^{120}$Sn(p,n)$^{120}$Sb reaction. The measurement of *Johnson et al* [16] (squares) covers the (3.7-7.0) MeV range of the incident energies and *Lovchikova et al* [17] give the points (triangles) of the

**Figure 1**. Excitation functions (left column), astrophysical S-factors (middle column) and reaction rates (right column) for $^{115}Sn(p,n)^{115}Sb$ (upper row), $^{116}Sn(p,n)^{116m+g}Sb$ (middle row) and $^{120}Sn(p,n)^{120m+g}Sb$ (lower row). Points are the experimental values, curves are the statistical theory predictions. The arrows on the plots in the left column show the reaction thresholds. The rates were computed by different combinations of data and theory (see text).

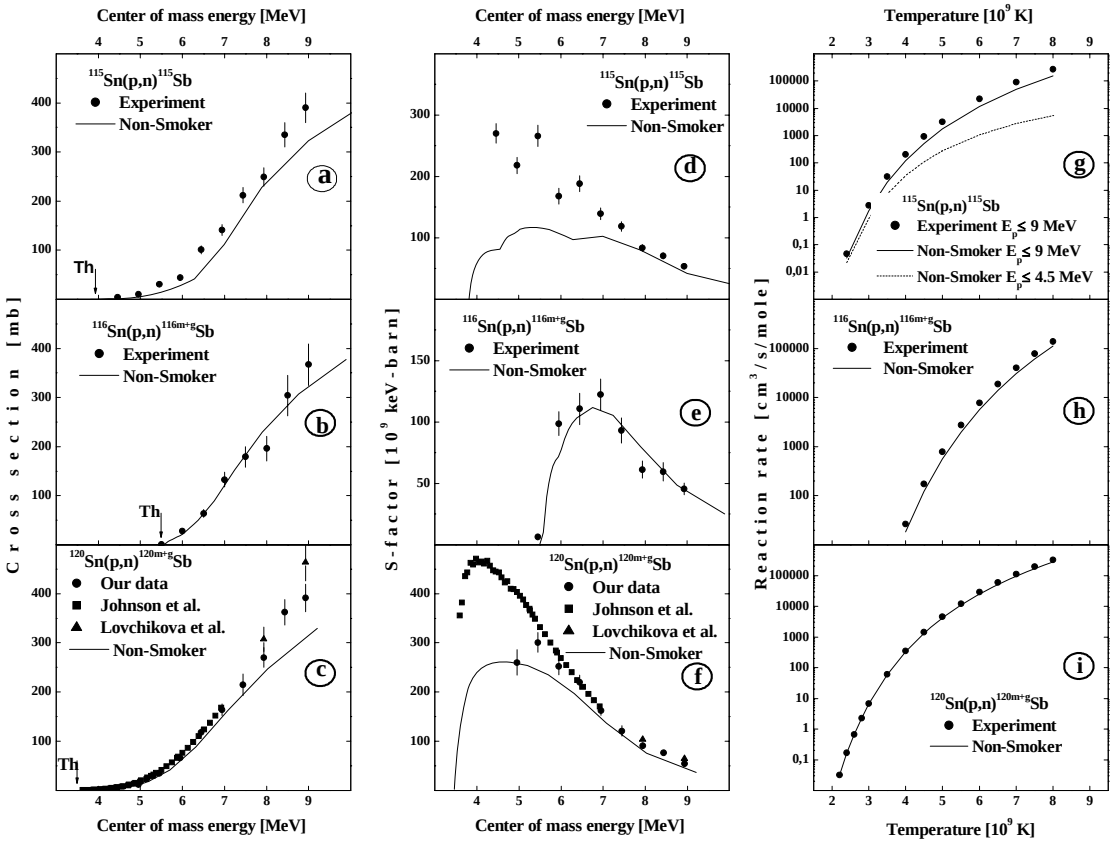


measured cross sections at 8 and 9 MeV. Both of these teams had measured the cross sections by counting the emitted neutrons. While there is acceptable agreement within errors between our measurement and the *Johnson et al* data above about 6.5 MeV, our data indicate smaller cross sections and S-factors at lower energies (see graphs *c* and *f* of Figure 1).

The total cross sections $\sigma(E)$ of the (p,n)-reactions studied were transformed to astrophysical S-factors $S=E\sigma(E)e^{2\pi\eta}$. Here, $E$ is the center-of-mass energy, $\eta=Z_1Z_2e^2/h\upsilon$ is the Sommerfeld parameter with $Z_1$ and $Z_2$ as the charge numbers of interacting particles and $\upsilon$ their relative velocity. The S-factors for our reactions are given in the middle column of Figure 1. A reasonable agreement between theoretical predictions and our experimental values of S-factors is found for $^{116}Sn(p,n)^{116}Sb$ and $^{120}Sn(p,n)^{120}Sb$ in the whole energy range studied and for $^{115}Sn(p,n)^{115}Sb$ at the higher energy range. However, theory underestimates the S-factor values for the $^{115}Sn(p,n)^{115}Sb$ reaction at low energies. The discrepancy between the *Johnson et al* data and our measurement for $^{120}Sn(p,n)^{120}Sb$ can be clearly seen in the S-factor plot. The theoretical values agree better with the new data.

As quantities of primary astrophysical interest, the experimental and theoretical reaction rates were calculated for different temperatures *T* from the cross section values using the known expression:

$$N_A\langle\sigma\upsilon\rangle = \left(\frac{8}{\pi\mu}\right)^{1/2} \frac{N_A}{(k_B T)^{3/2}} \int_{E_{th}}^{\infty} \sigma(E)\exp(-\frac{E}{k_B T})dE,$$

where $N_A$ is the Avogadro number, μ the reduced mass of the system, $k_BT$ the thermal energy with $k_B$ being the Boltzmann constant. To perform the integration, our experimental data was interpolated polynomially unless otherwise specified below.

The threshold of the $^{115}$Sn(p,n)$^{115}$Sb reaction is at 3.85 MeV. It means that this reaction can contribute to nucleosynthesis at stellar plasma temperatures $T=2.4\times10^9$ K and more since the Gamow window starts to cover the reaction threshold at this temperature. The high energy limit of our measurements (9 MeV) corresponds to the edge of Gamow window at $8\times10^9$ K. That is why the experimental values of this reaction rate shown as the points on graph *g* of Figure 1 are displayed in this temperature interval. For the calculation of the reaction rates in the energy region 3.85-4.5 MeV we used the theoretical values of the cross sections normalized to the low energy experimental points because we have no experimental data for $E_p<4.5$ MeV. The purely theoretical reaction rates are presented by the solid curve. The dashed curve shows the contribution of the 3.85-4.5 MeV energy interval to the reaction rate at different temperatures. It contributes about ~68% at $T=2.4\times10^9$ K (which is relevant for the p-process) and 3.6 % at $T=8\times10^9$ K. Further experimental cross sections are needed near the threshold. Theory (solid curve) underestimates the reaction rate by about ~43% at the temperature $8\times10^9$ K.

Since the threshold of the reaction $^{116}$Sn(p,n)$^{116}$Sb is higher, being 5.54 MeV for the ground state, the temperature region in which the reaction rates can be calculated from our experimental data is $(4.0\text{-}8.0)\times10^9$ K. The results are given by points in graph *h* of Figure 1. The theoretical predictions are depicted by the curve. They underestimate the reaction rates by about 30% for $T=4\times10^9$ K and 20% for $T=8\times10^9$ K.

Analogous to the previous reactions, reaction rates were calculated for the $^{120}$Sn(p,n)$^{120}$Sb reaction utilizing the H-F prediction for the low incident proton energies. The experimental and theoretical results obtained in the temperature region $(2.2\text{-}8.0)\times10^9$ K are presented by the points and the curve, respectively, in graph *i* of Figure 1. The theory underestimates the reaction rate by 15% at the high temperature end. Obviously, theoretical and experimental rate coincide at the lowest plotted energy.

## 4. Conclusion

Measurements and analysis of the cross sections of (p,γ)- and low threshold (p,n)-reactions are of interest to supplement data sets for nuclear astrophysics and to test H-F predictions.

Excitation functions of the reactions $^{115}Sn(p,n)^{115}Sb$, $^{116}Sn(p,n)^{116m,g}Sb$ and $^{120}Sn(p,n)^{120m,g}Sb$ were measured at incident beam energies from 4.5 to 9.0 MeV using the activation technique. A reevaluation of the total cross sections was performed and compared with statistical model predictions and literature data. A remarkable difference between the experimental and theoretical values are observed only for the low-energy part of the $^{115}Sn(p,n)^{115}Sb$ reaction. There is also some discrepancy between *Johnson et al* [15] and our experimental results for the low-energy part of $^{120}Sn(p,n)^{120}Sb$. Reaction rates were derived by combining data and theory.

## References


[1] E. Burbidge, G. Burbidge, W. Fowler and F. Hoyle, *Rev. Mod. Phys.* **29**, 547 (1957).

[2] C. Angulo et al. *Nucl. Phys.* **A656**, 3 (1999).

[3] http://nuclear-astrophysics.fzk.de/kadonis/ .

[4] T. Rauscher. NON-SMOKER library, http://nucastro.org/reaclib.html.

[5] J. Cowan, F.-K. Thielemann and J. Truran. *Phys. Rep.* **208**, 267 (1991).

[6] T. Rauscher, F.-K. Thielemann. *Nucl. Data Tables.* **75**, 1 (2000); **79**, 1 (2001).

[7] S. Goriely. In: *S. Wender (Ed.), Proc. Capture Gamma-Ray Spectroscopy and Related Topics*, in: *IOP Conference Proceedings*, **Vol. 529**, 287 (2000). (see also http://www-astro.ulb.ac.be).

[8] V.G. Batij, E.A. Skakun, *40. Conf. Nucl. Spectroscopy Nucl. Struct.*, Leningrad 1990 p.273. Accessions A0617005, A00617006 in EXFOR-base.

[9] A.P. Kljucharev, L.I. Kovalenko, L.G. Lishenko, V.N. Medjanik, T.S. Nazarova,., A.A Rozen, *Thin Foils of Metal Isotopes. Preparation Methods. Energoizdat*, Moscow, USSR (1981).

[10] V.A. Bomko et al. *Particle Accelerators* **6**, 1 (1974).

[11] C.F. Williamson, J.P. Boujot, J. Picard, *Tables of Range and Stopping Power of Chemical Elements for Charged Particles of Energy 0.05 to 500 MeV*. Report CEA-R-3042, Saclay, France (1966).

[12] http://nds121.iaea.org/ensdf/, http://www-nds.iaea.org/nudat,

http://nucleardata.nuclear.lu.se/nucleardata/toi/.

[13] F.R. Chloupek et al. *Nucl. Phys.* **A652**, 391 (1999).

[14] N. Özkan et al. *Nucl. Phys.* **A710**, 469 (2002).

[15] E. Brown, R.B. Firestone, *Table of Radioactive Isotopes*. John Wiley & Sons, New York (1986).

[16] C.H. Johnson et al. *Phys. Rev.* **C2**, 639 (1970); **C15**, 196 (1977).

[17] G.N. Lovchikova et al. Sov.J.Nucl.Phys. **31**, 1 (1980).